RESEARCH ARTICLE

A thermophilic hormone-sensitive lipase family esterase Est1404 identified from an Antarctic bacterium *Pseudomonas* sp. E2-15

Yuanfang He,[1] Rui Deng,[2] Xiaoyu Liu,[1] Shu Xing,[1] Xiying Zhang,[3] Hailun He,[4] John Kevin Bielicki[1] & Mingyang Zhou[1]

[1]School of Chemistry and Chemical Engineering, Qilu University of Technology (Shandong Academy of Sciences), Jinan, PR China; [2]School of Bioengineering, Qilu University of Technology (Shandong Academy of Sciences), Jinan, PR China; [3]State Key Laboratory of Microbial Technology, Marine Biotechnology Research Center, Shandong University, Qingdao, PR China; [4]State Key Laboratory of Medical Genetics, School of Life Sciences, Central South University, Changsha, PR China

Abstract

Esterases are a group of enzymes with a diverse range of uses in industry. We identified a novel hormone-sensitive lipase (HSL) in the esterase family, Est1404, through cloning and expression from the Antarctic bacterium *Pseudomonas* sp. E2–15, from soil collected on King George Island. Investigations showed that the Est1404 enzyme is a thermophilic esterase that maintains 90–100% activity throughout the temperature range of 60–90 °C. It exhibits the highest catalytic activity towards *p*-nitrophenol butyrate at 70 °C and pH 8.5. Est1404 was inhibited by the serine-modifying reagent phenylmethylsulfonyl fluoride, but thiol reagents such as dithiolthreitol stimulated its activity. Metal chelating chemicals, such as ethylenediaminetetraacetic acid, did not affect its activity. Phylogenetic analysis indicated that Est1404 is in the GDSAG subfamily of HSL. The enzyme contains a GDSAG motif with an active serine (S) positioned within a catalytic triad consisting of highly conserved Ser^{156}, Asp^{250} and His^{280} residues. The thermal stability of the Est1404 esterase makes it potentially useful in industrial catalysis.

Keywords

Antarctica; bacteria; enzyme; HSL family

Correspondence

Mingyang Zhou, School of Chemistry and Chemical Engineering, Qilu University of Technology (Shandong Academy of Sciences), No. 3501 Daxue Road, Changqing District, Jinan 250353, Shandong Province, PR China. E-mail: myzhou@qlu.edu.cn

Abbreviations

CTAB: cetyltrimethylammonium bromide
DMF: *N*, *N*-dimethylformamide
DMSO: dimethyl sulfoxide
DTT: dithiothreitol
EDTA: ethylenediaminetetraacetic acid
HSL: hormone-sensitive lipase
kDa: kilodalton
PCR: polymerase chain reaction
pI: theoretical isoelectric point
PMSF: phenylmethylsulfonyl fluoride
*p*NP: *p*-nitrophenyl esters
SD: standard deviation
SDS: sodium dodecyl sulfate
SDS-PAGE: sodium dodecyl sulfate–polyacrylamide gel electrophoresis
v/v: volume of liquid solute in a total volume of liquid
w/v: weight of solid solute in a total volume of liquid

Introduction

Esterase (EC3.1.1.1) and lipase (EC3.1.1.3) are classified as lipolytic enzymes on account of their ability to facilitate the hydrolysis and synthesis of ester linkages. A large number of enzymes are classified within the *α/β* hydrolase superfamily and exhibit a conserved GXSXG-pentapeptide motif close to the catalytic serine residue (Jochens et al. 2011; Kovačić et al. 2018). Lipases hydrolyse water-insoluble long-chain acyl substrates, show interfacial activation and are thereby distinguished from esterases (Bornscheuer 2002). Esterases often facilitate the hydrolysis of ester substrates with short carbon chains and exhibit traditional Michaelis-Menten kinetics. Lipolytic enzymes exhibit broad substrate specificity, chiral selectivity and organic reagent tolerance (Rong et al. 2018), making them exceptionally versatile biocatalysts. Their unique properties enable diverse industrial applications, including detergent formulations, food flavour modification and stereoselective pharmaceutical synthesis (Bredai et al. 2021; Reyes-Reyes et al. 2022; Sharma et al. 2024). This remarkable functional adaptability arises from evolutionarily optimized molecular architectures that strike a balance between substrate promiscuity and catalytic precision.

Citation: *Polar Research* 2026, *45*, 10747, http://dx.doi.org/10.33265/polar.v45.10747

On the basis of their optimal activity temperatures, enzymes are categorized into four groups: psychrophilic enzymes, which exhibit maximum activity at low temperatures ranging from 5 to 25 °C; mesophilic enzymes, functionally optimized for moderate temperatures between 25 and 50 °C; thermophilic enzymes, which demonstrate peak activity above 60 °C and display high thermostability at elevated temperatures and hyperthermophilic enzymes, which exhibit optimal activity above 80 °C (Bruins et al. 2001; Vieille & Zeikus 2001). These differences reflect fundamental mechanisms of protein thermal adaptation. Cold-adapted enzymes gain structural flexibility and high catalytic efficiency at low temperatures by reducing weak interactions such as salt bridges, hydrophobic contacts and disulfide bonds. Their active sites are typically more open and dynamic, with greater substrate accessibility and higher local flexibility facilitated by small amino acid residues (Feller et al. 1992; D'Amico et al. 2006; Feller 2013). In contrast, thermophilic and hyperthermophilic enzymes achieve extreme thermal stability through enhanced structural rigidity. This is enabled by additional hydrogen bonds, optimized salt bridges, stronger hydrophobic clustering and metal ion coordination, which collectively suppress thermal unfolding and denaturation (Li et al. 2005; Corazza et al. 2006). This structural trait confers exceptional stability and performance at high temperatures, which is a key biotechnological advantage.

Lipolytic enzymes are found in animals, plants, fungi and microorganisms (Zhang et al. 2017; Wang et al. 2018; Yu et al. 2018; Zhang et al. 2018; Arnling Bååth et al. 2019; Curci et al. 2019; Kim et al. 2019; Mogodiniyai Kasmaei & Sundh 2019; Tutuncu et al. 2019). Many enzymes' genes were successfully obtained from metagenomes and bacterial sources, such as enzymes exhibiting diverse biological activities isolated from *Pseudomonas* Zhang et al. 2017), *Psychrobacter* (Zhang et al. 2018), *Salinisphaera* (Kim et al. 2019), *Serratia* (Jiang et al. 2016), *Burkholderia* (Yang et al. 2016), *Bacillus* (Soumya & Kochupurackal 2022) and *Staphylococcus* (Zhao et al. 2021), which exhibit remarkable catalytic versatility. This microbial diversity takes on special significance in extreme environments such as Antarctica, where these enzymes play pivotal roles in maintaining ecosystem function through organic matter turnover and nutrient cycling (Lima et al. 2022). The evolutionary distinctiveness of Antarctic microbial communities suggests that their lipolytic enzymes may possess unique adaptive features not found in temperate species (Ashaolu et al. 2025).

Arpigny & Jaeger (1999) have classified bacterial lipolytic enzymes into eight distinct families. The fourth family, the HSL family, exhibits amino acid sequence similarity to human HSL (Arpigny & Jaeger 1999). The HSL family exhibits greater stability and a broader range of substrate specificity compared to other families. The catalytic triad of Ser-His-Asp residues constitutes the active site of the HSL relatives. Most esterases and lipases within the HSL family have a catalytic Ser inside the largely conserved motif, denoted as G-X-S-X-G (Kim 2017; Le et al. 2019). Bacterial HSL family esterase molecules are categorized into three distinct subfamilies based on the presence of specific motifs, such as GDSAG or GTSAG motif (Li et al. 2014). The Antarctic bacterium *Pseudomonas* sp. E2–15 demonstrates remarkable adaptability to extreme cold conditions and has proven to be a valuable source of novel lipolytic enzymes. Our previous work characterized Est19, a cold-adapted esterase belonging to the HSL family from this strain. Based on phylogenetic analysis and biochemical characterization, we established the third subfamily of the HSL family, which possesses the GESAG motif represented by Est19 (Liu, Zhou et al. 2021).

Here, we identified the esterase gene *est1404* from the genome of *Pseudomonas* sp. E2–15 and, we recombinantly produced and purified the esterase for its analysis. The results suggest that Est1404 is a member of the HSL family. Unlike the cold-adapted enzyme Est19, enzyme Est1404 is a thermophilic enzyme.

Methods

Bacterial strain

The gene encoding the target esterase was sourced from *Pseudomonas* sp. strain E2–15, isolated from a permafrost soil sample taken from King George Island, South Shetland Islands (62°11'17.5"S, 58°55'23.4"W; Liu, Liu et al. 2021). For isolation, 1 g of soil was suspended and serially diluted, plated on skim milk agar and incubated at 15 °C. A colony forming a prominent clear zone (hydrolytic halo) was subcultured repeatedly on fresh plates of the same medium to obtain a pure culture, which was designated as strain E2–15.

Sequence, phylogenetic and structural analyses

The whole genome shotgun sequencing project of the source strain, *Pseudomonas* sp. E2–15, has been deposited at GenBank and at the National Genomics Data Center of the Beijing Institute of Genomics (see Data availability section). The *est1404* gene was identified within this genomic assembly, and its specific coding sequence has been assigned the GenBank accession number OR876274.

The molecular weight and pI of the esterase were predicted using the ExPASy database (Gasteiger et al. 2005), and a probable signal peptide was identified using SignalP

Citation: *Polar Research* 2026, *45*, 10747, http://dx.doi.org/10.33265/polar.v45.10747

server 5.0 (Almagro Armenteros et al. 2019). The AlphaFold2 platform (https://www.alphafold.ebi.ac.uk/) was utilized to forecast the structures of Est1404 and Est19. The predicted structures were further analysed using CASTpFold (Ye et al. 2024) for pocket volumetry and ProteinTools (Ferruz et al. 2021) for hydrogen bond network analysis. The alignment of sequences was performed using ClustalX (Jeanmougin et al. 1998) and ESPript 3.0 (Robert & Gouet 2014). A maximum likelihood phylogenetic tree was produced using the Mega version 11.0.13 (Tamura et al. 2021). Reference sequences were curated from the ESTHER database to encompass high-confidence, representative and full-length members of both major HSL subfamilies (defined by GDSAG and GTSAG motifs) across diverse bacterial taxa. The tree was generated using the maximum likelihood method based on the JTT matrix-based model.

Cloning, expression and purification of recombinant Est1404

The primers *est1404F* (5′-AAGAAGGAGATATACATATGCG Catgtacccgatttctccgca-3′) and *est1404R* (5′-TCGAGTGCGG CCGCAAGCTTgacctgtgtcagccgctcgctcc-3′) amplified the gene *est1404* (GenBank accession number OR876274) from the genome of *Pseudomonas* sp. E2–15, which contained *Hind*III and *Nde*I digestion sites (underlined). The nucleotides that paired with the vector sequence were displayed in capital characters, whilst the esterase gene sequence was in lowercase letters. The PCR product, after purification, was cloned into the pET-22b (+) vector (Novagen, USA) digested by *Hind*III and *Nde*I enzymes, employing the M5 Compact Seamless Assembly and Cloning Mix Kit (Mei5bio, China). The recombinant plasmid was introduced into chemically competent *Escherichia coli* BL21 (DE3) cells by heat shock (42 °C for 90 seconds) and subsequently incubated in LB broth at 37 °C for one hour. The transformed cells were then plated on LB agar containing 100 μg/mL ampicillin. Plasmid integrity was verified by DNA sequencing.

For protein expression, a culture of *Escherichia coli* BL21 (DE3), containing the recombinant plasmid, was grown in LB medium containing 100 μg/ml ampicillin at 37 °C. When the optical density at 600 nm reached 0.6–0.8, the expression was induced by adding isopropyl β-D-1-thiogalactopyranoside at a final concentration of 0.1 mM. The cells were then cultured for 24 hours at 15 °C and 120 rpm.

Cells were centrifuged at 10 000 × g for 10 minutes (4 °C). Subsequently, the cell pellet was rinsed three times using a solution of Tris-buffered saline (50 mM Tris-HCl, 100 mM NaCl, pH 8.0), and cells were disrupted by sonication using a JY92-II ultrasonic cell disruptor (Ningbo Scientz Biotechnology) at 60% amplitude with three-second pulses followed by two-second intervals for 15 minutes. A crude extract was obtained by centrifugation at 11 000 × g for 30 minutes at 4 °C, and the supernatant (soluble fraction) was used for further procedures after confirming target protein presence by SDS-PAGE analysis of both soluble and insoluble fractions. The esterase protein was purified by immobilized metal affinity chromatography using Ni-Sepharose Fast Flow resin (GE Healthcare, USA) at 1 mL resin per 24 mg protein. The binding buffer contained 50 mM Tris-HCl, 100 mM NaCl and 5 mM imidazole (pH 8.0). After equilibrating the column with binding buffer, the sample was loaded. Unbound proteins were then washed away using the binding buffer (50 mM Tris-HCl, 100 mM NaCl, 5 mM imidazole, pH 8.0). Stepwise elution was performed using buffers containing 50 mM Tris-HCl, 100 mM NaCl with increasing imidazole concentrations (50 mM, 100 mM and 250 mM, pH 8.0). The eluted protein was dialysed against 50 mM Tris-HCl (pH 8.0) to remove imidazole and salt. The purity of the protein was assessed using SDS-PAGE with 12% resolving gel and 4% stacking gel (Laemmli system), stained with Coomassie Brilliant Blue R-250. Total protein concentration was determined by Bradford assay using bovine serum albumin as standard. The N-termini sequencing was conducted by a commercial company (Biotech-Pack, China).

Esterase assay

The measurement of esterase and lipase activity was conducted using the methodology described by Li et al. (2014). The *p*-nitrophenyl (*p*NP) ester substrates (acetate, C2; butyrate, C4; caproate, C6; caprylate, C8; caprate, C10; laurate, C12; palmitate, C16) were prepared as 10 mM solutions in 2-propanol. The standard reaction system consisted of 0.02 ml of 10 mM *p*NP-C4, 0.02 ml of enzyme (1.54 mg/ml total protein concentration) and 0.96 ml of 50 mM Tris-HCl buffer (pH 8.0). The reaction was stopped by adding 0.1 ml of 20% SDS (w/v) after incubating at 70 °C for 10 minutes. The absorbance at a wavelength of 405 nm was measured for *p*-nitrophenol quantification. One unit of enzyme was defined as the quantity of enzyme needed for releasing 1 μmol of *p*-nitrophenol per minute. The blank control was prepared by replacing the enzyme with 0.02 ml of buffer in the identical reaction setup. Specific activity was expressed as units per milligram of protein.

The substrate specificity was assessed using *p*NP esters, including C2, C4, C6, C8, C10, C12 and C16. The optimal temperature was evaluated over a range of 0 to 100 °C, with increments of 10 °C. The optimal pH was evaluated using Britton-Robinson buffer (Piroozmand et al. 2020), ranging from pH 4 to 11, with increments of 1 or 0.5, at a

temperature of 70 °C. To investigate the thermal stability of the enzyme, Est1404 was subjected to incubation at temperatures of 40, 70 and 95 °C for 120 minutes. The remaining activity of the enzyme was then measured at 15-minute intervals. All assays incorporated blank controls using buffer in place of enzyme to account for spontaneous hydrolysis. Experiments were performed in triplicate, with the highest activity under optimal conditions was defined as 100% for relative activity calculations. All experiments were performed with three biological replicates, each with three technical replicates. Data are presented as the mean ± SD of the biological replicates.

The kinetic parameters of Est19 and Est1404 were determined using *p*-nitrophenyl caproate (*p*NP-C6) as the substrate. Assays were conducted in 50 mM Tris-HCl buffer (pH 8.0) at 40 °C, with substrate concentrations ranging from 0.01 to 4.0 mM. The Michaelis–Menten equation was fitted to the experimental data by nonlinear regression using GraphPad Prism software (version 8.0.2 for Windows) to derive the kinetic parameters K_m, V_{max}, k_{cat} and k_{cat}/K_m.

The effect of additives on Est1404 activity

The impact of possible inhibitors, chemical solvents and metal ions on the activity of Est1404 was assessed using the *p*NP-C4 substrate. The additive concentrations were selected based on the characterization methods reported for similar esterases (Li et al. 2014; Li et al. 2020). The putative inhibitors PMSF, EDTA, DTT and CTAB were evaluated at final concentrations of 1 and 10 mM, while SDS and Tween-80 were assessed at concentrations of 1 and 10% (w/v), respectively. The impact of several organic solvents was assessed by adding methanol, formaldehyde solution, ethanol, acetonitrile, acetone, isopropyl alcohol DMSO and DMF at final concentrations of 20 and 40% (v/v). The enzyme activity, in the absence of any additions, was established as 100%.

Results

Sequence analysis

The *est1404* gene, located in Scaffold 6 of the whole genome shotgun assembly with GenBank accession number JBSKFM010000006.1, comprised a 951 bp open reading frame encoding a 316-amino acid precursor protein, with the mature protein containing 311 amino acids after processing. Bioinformatic analysis predicted a protein molecular weight of 33.5 kDa and a theoretical pI of 5.08. No signal sequence was identified in Est1404 by SignalP analysis. The Protein BLAST analysis conducted at the National Center for Biotechnical Information (US National Institutes of Health) revealed that the initial 100 amino acids of the sequence with the greatest similarity were all derived from an uncharacterized protein annotated from the bacterial genome sequences. Based on the phylogenetic tree, the protein has been categorized as belonging to the HSL family (Fig. 1).

The multiple-sequence alignment of Est1404 with its related proteins identified a catalytic triad consisting of Ser^{156}, Asp^{250} and His^{280} residues (Fig. 2). The catalytic Ser^{156} was found within a conserved motif GDSAG, indicating its membership in the GDSAG subfamily. The amino acid sequences of Est1404 contained both the HSL family signature sequence HGGG and the recently discovered Y RNA-like A motif (Stivala et al. 2011). The structure predicted by the AlphaFold revealed that Est1404 exhibits a typical α/β hydrolase structure consisting of eight β-sheets and nine α-helices (Fig. 3). Structural comparisons between Est1404 and Est19 revealed that Est1404 possesses a significantly more compact catalytic pocket (Fig. 4), with its surface area measuring 518.968 Å² compared to 588.454 Å² in Est19, and a substantially smaller active site volume of 370.049 Å³ in Est1404 compared to 600.471 Å³ in Est19. Furthermore, Est1404 maintains an enhanced hydrogen bond network with 20 interactions compared to 18 in Est19 (Table 1). These structural features are consistent with Est1404's observed thermostability and catalytic efficiency at elevated temperatures.

Preparation of esterase Est1404

The *est1404* gene together with a sequence of a histidine tag at the C-terminus was ligated into the pET-22b (+) vector. The vector construct was introduced into *E. coli* BL21 (DE3) for expression. The SDS-PAGE analysis of the crude cell lysate indicated that the recombinant Est1404 was predominantly produced in the soluble fraction, with a minor portion present in inclusion bodies (Fig. 5). The expressed protein was purified using Nickel-affinity chromatography. The molecular weight of the purified protein was approximately 35 kDa (Fig. 5), which is consistent with the expected molecular weight. Sequencing the N-termini revealed that the first amino acid residue Met^1 was removed when expressed in *E. coli*. This processing is consistent with *E. coli*'s native post-translational modification system where methionine aminopeptidase removes the initiator methionine. The purified enzyme showed a specific activity of 2840 units/mg.

Characteristics of Esterase Est1404

The substrate selectivity of Est1404 was assessed by employing *p*NP with varying acyl chain lengths. Among

Citation: *Polar Research* 2026, *45*, 10747, http://dx.doi.org/10.33265/polar.v45.10747

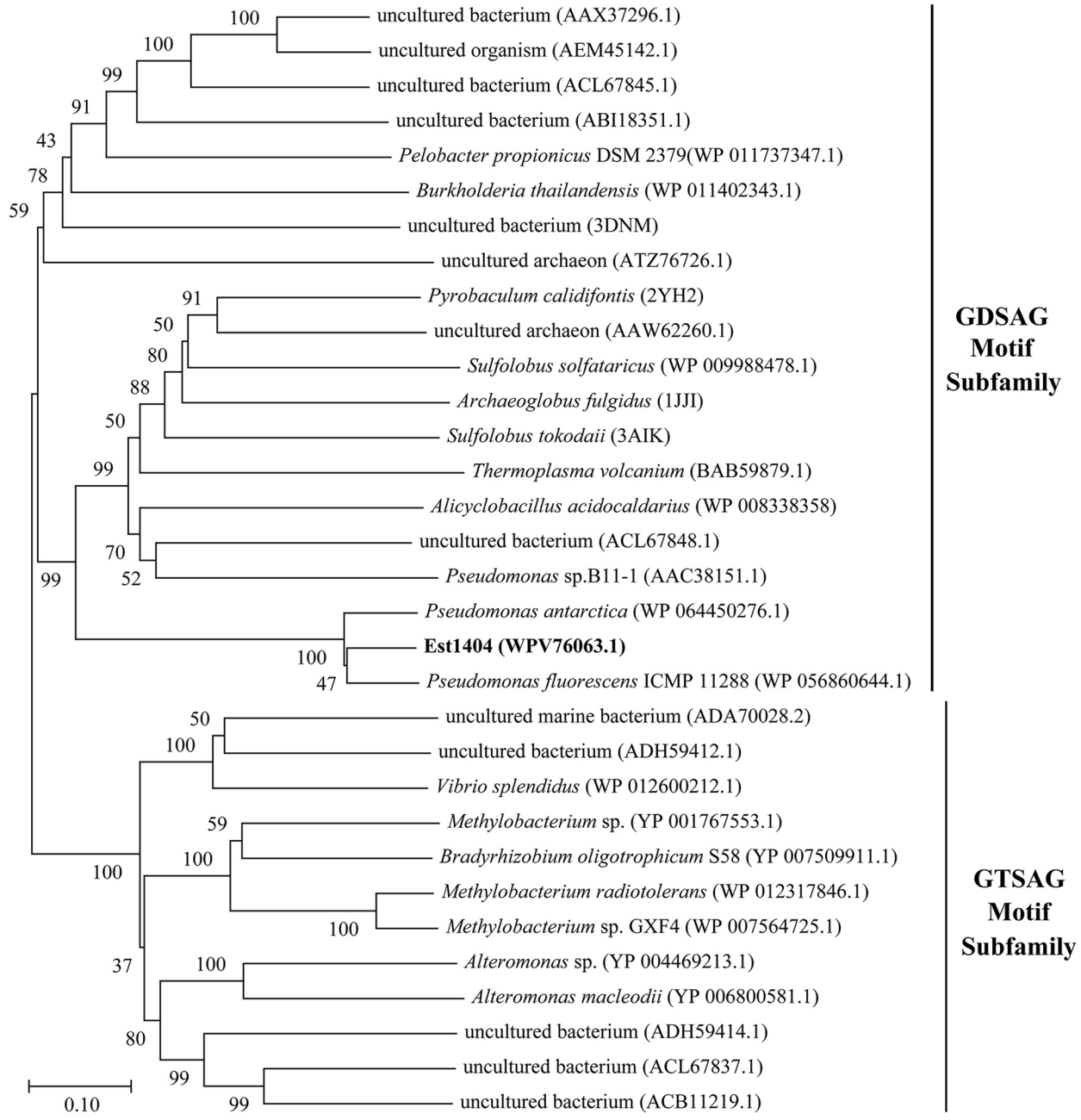

Fig. 1 Phylogenetic analysis of Est1404. The tree was constructed using the Maximum Likelihood method based on the JTT matrix-based model. Bootstrap analysis of 1000 replicates were conducted and only values above 50% are shown.

these esters, the enzyme exhibited the greatest hydrolytic activity towards *p*NP-C4 (Fig. 6a). However, a drastic decrease in activity was observed for substrates longer than C6, becoming negligible for *p*NP-C8, *p*NP-C10, *p*NP-C12 and *p*NP-C16. This sharp decline is likely attributed to steric hindrance within the enzyme's active site, where the limited space in the acyl-binding pocket cannot accommodate the longer aliphatic acyl chains of C8 and above. These results indicated that Est1404 was an esterase rather than a lipase.

The impact of temperature and pH on esterase activity was quantified using *p*NP-C4 (Fig. 6b, c). These findings indicated that the optimum conditions for activity determination were a temperature of 70 °C and pH 8.5.

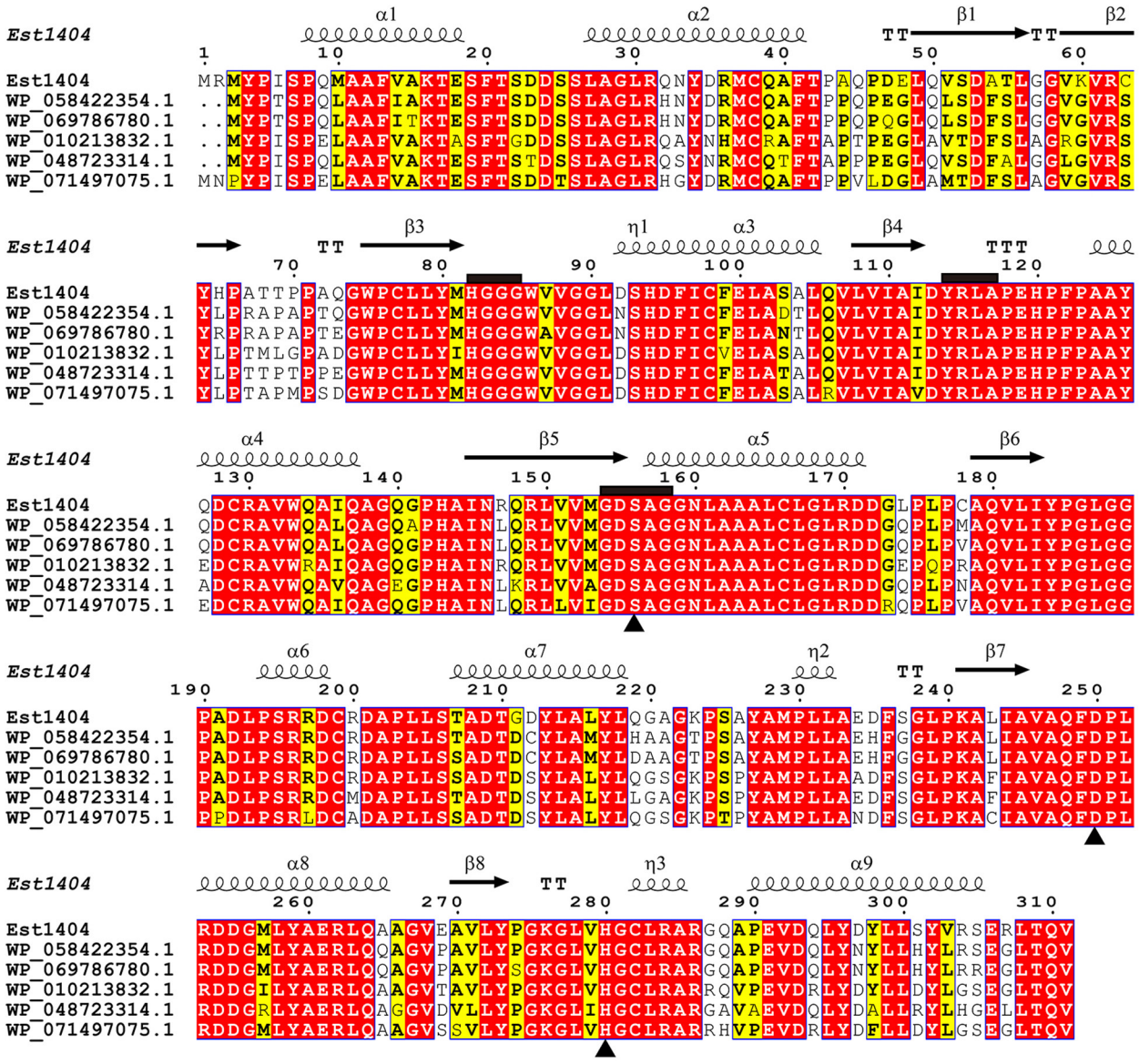

Fig. 2 Sequence alignment of Est1404 and its analogs. Identical residues are shown in white on a red background, and similar residues (homology ≥75%) are on a yellow background. Black triangles indicate residues forming the catalytic triad Ser, Asp and His. Black rectangles indicate conserved motifs.

Approximately 70% of the maximum activity of Est1404 was maintained across a broad temperature range spanning from 60 to 90 °C. Notably, Est1404 maintained approximately 65% of its activity hydrolysing *p*NP-C4 at a temperature of 100 °C.

In order to investigate the thermal stability of the enzyme, Est1404 was subjected to temperatures of 40, 70 and 95 °C for 120 minutes of incubation, before its activity was determined (Fig. 6d). The results of these studies indicated that Est1404 exhibited significant stability at temperatures of 40 and 70 °C, retaining nearly all of its activity after incubation at these high temperatures. Incubation of Est1404 at 95 °C for 45 minutes resulted in a 20% decrease in activity; however, the remaining 80% activity was stable for up to two hours. Collectively, these results suggested that Est1404 was a thermophilic esterase.

The esterase Est19 exhibited a Michaelis constant (K_m) of 147 ± 28 μM, a maximum reaction rate (V_{max}) of 37 423 ± 2478 μM/min/mg, and a turnover number (k_{cat}) of 21.86 ± 1.45 s^{-1}. The catalytic efficiency (k_{cat}/K_m) of Est19 was calculated to be 148.68 $s^{-1}mM^{-1}$. In contrast, the

Citation: *Polar Research* 2026, *45*, 10747, http://dx.doi.org/10.33265/polar.v45.10747

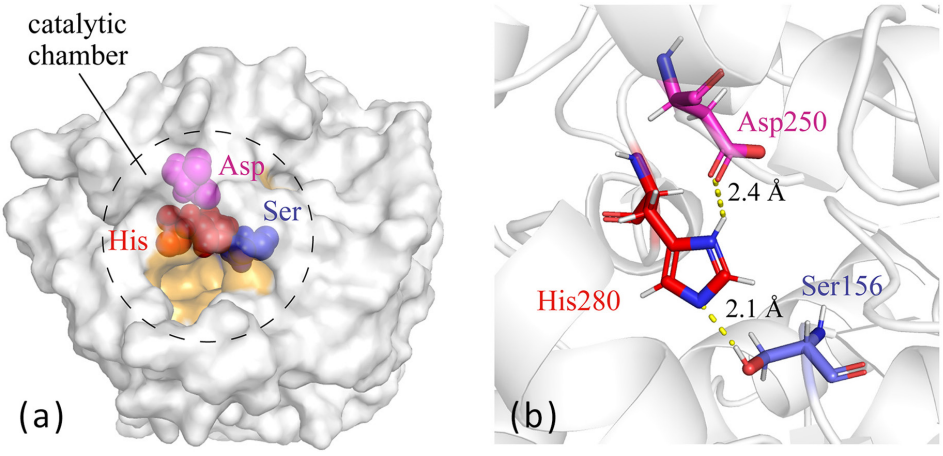

Fig. 3 Predicted structure of Est1404. (a) The three-dimensional model of Est1404 was generated using AlphaFold2, and the optimal structure was visualized using PyMOL. The binding pocket surface is highlighted in orange. Key catalytic residues are represented as spheres: histidine (red), serine (blue) and aspartate (magenta). (b) Structural analysis of Est1404 revealed a canonical catalytic triad comprising Ser^{141} (nucleophile), Asp^{275} (charge relay) and His^{303} (proton carrier) within its active site. The measured distances between Ser^{141}–His^{303} and His^{303}–Asp^{275} are 2.1 Å and 2.4 Å, respectively.

thermostable esterase Est1404 showed a significantly higher K_m value of 187 ± 24 μM, indicating a lower substrate binding affinity compared to Est19. The V_{max} and k_{cat} values for Est1404 were 4026 ± 58 μM/min/mg and 1.47 ± 0.19 s^{-1}, respectively, both substantially lower than those of Est19. Consequently, the catalytic efficiency (k_{cat}/K_m) of Est1404 was 7.9 $s^{-1}mM^{-1}$, which is lower than that of Est19 (Table 1).

The effect of inhibitors and organic solvents on Est1404 activity

Consistent with the presence of a catalytic triad of Ser-Asp-His, the esterase activity of Est1404 was significantly reduced by the serine-modifying reagent PMSF, as shown in Table 2. The metal ion chelator, EDTA, did not have any influence on the activity of Est1404, indicating that the enzyme does not rely on metal ions for its functionality. Conversely, the thiol reagent, DTT, significantly enhanced (by 300–400%) the activity of Est1404. In contrast, ionic (SDS) and non-ionic (Tween80) detergents inactivated the enzyme, suggesting that disruption in hydrophobic interactions resulted in the loss of structural integrity of the enzyme. The presence of CTAB resulted in a modest but notable enhancement (50–70%) of Est1404 activity.

Table 2 also shows the effect of various solvents on the enzymatic activity of Est1404. The enzyme was found to be largely unaffected by solvents such as alcohols. Incubations of Est1404 with upwards of 20% methanol or ethanol did not affect the enzyme activity. The solvents acetone, isopropanol and DMF had a moderate impact on Est1404 activity when employed in high concentrations. However, the organic solvents acetone at 20% and 40%, resulted in 40% and 78% reductions in activity, respectively. Similarly, Est1404 exhibited poor tolerance for both acetonitrile and DMSO, with 40% acetonitrile causing almost total inhibition of the enzyme. The enzyme was nearly completely deactivated by 20–40% formaldehyde, consistent with its known protein-crosslinking effects (Liu et al. 2011), confirming Est1404's susceptibility to irreversible covalent modification.

Discussion

Our laboratory studies bacteria from soil samples taken from Antarctica to identify gene products that may be useful for commercial applications. As part of these ongoing studies, a novel esterase gene, *est1404*, was identified from the genome of a bacterial strain, *Pseudomonas* sp. E2-15, that has not been previously described. Protein BLAST analysis indicated the gene product had the greatest similarity to uncharacterized *α/β* hydrolases. The isolated protein was found to be a serine hydrolase with unique attributes, including the ability to retain enzymatic activity at high temperatures for prolonged periods. We undertook further studies to characterize the substrate specificity and biochemical properties of this new esterase under various conditions.

The Est1404 esterase exhibited good catalytic efficiency towards *p*-nitrophenol esters. The substrate specificity of Est1404 was found to be very similar to that of several previously characterized esterases, such as Esterase Est11 obtained from the marine bacterium *Psychobacterium pacificensis* (Wu et al. 2015), Esterase

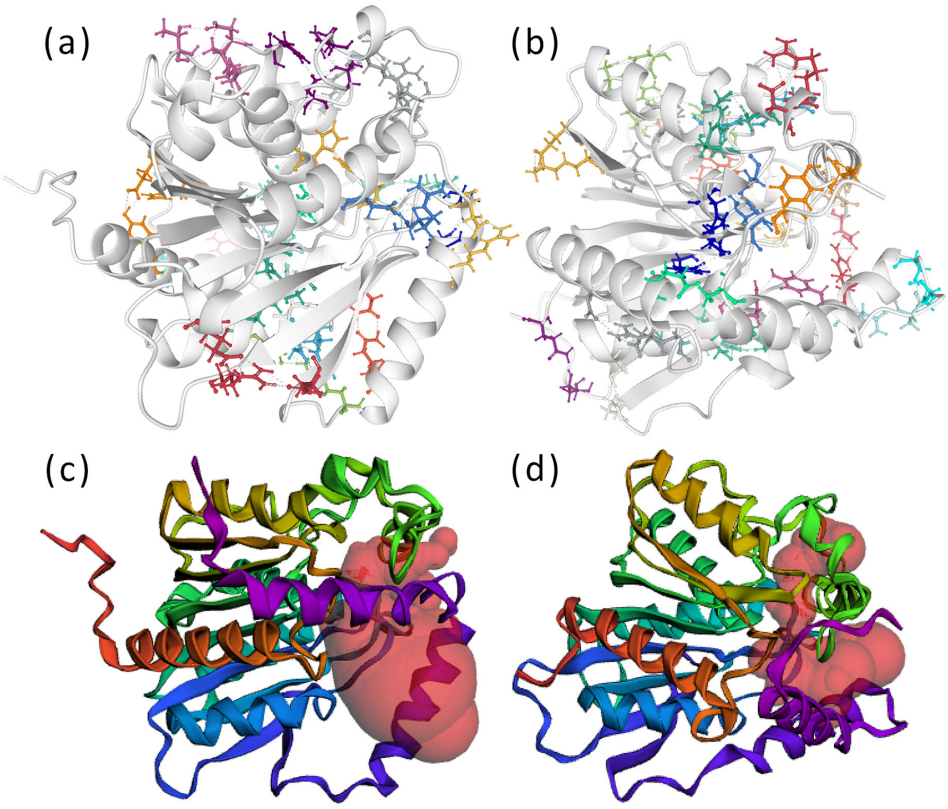

Fig. 4 Structural comparison of EST19 and EST1404. (a) Hydrogen-bonding network of Est19 predicted by ProteinTools, with participating residues shown as coloured sticks. (b) Hydrogen-bonding network of Est1404 predicted by ProteinTools, displayed similarly. (c) Binding pockets and cavities of Est19 identified by CASTp 3.0, with pockets highlighted in red. (d) Binding pockets and cavities of Est1404 identified by CASTp 3.0, displayed with the same colour scheme.

PMGL2 obtained from the permafrost metagenome (Petrovskaya et al. 2016) and Esterase H9Est obtained from the Tibetan glacier metagenomic library (De Santi et al. 2015). Like all of these esterases, Est1404 tends to

Table 1 Comparison of the enzymatic and structural properties of Est1404 and Est19. The enzymatic kinetic parameters presented in the table are expressed as mean SD, derived from three independent biological replicates, with each replicate consisting of three technical measurements.

Parameters	Est19	Est1404
Optimal temperature	40 °C	70 °C
Thermal stability	Low	High
K_m (μM)	147 ± 28	187 ± 24
V_{max} (μM/min/mg)	37423 ± 2478	4026 ± 58
k_{cat} (S^{-1})	21.86 ± 1.45	1.47 ± 0.19
k_{cat}/K_m ($S^{-1}mM^{-1}$)	148.68	7.9
Number of hydrogen bond networks	18	20
Binding pocket volume ($Å^3$)	600.471	370.049
Binding pocket surface area ($Å^2$)	588.454	518.968

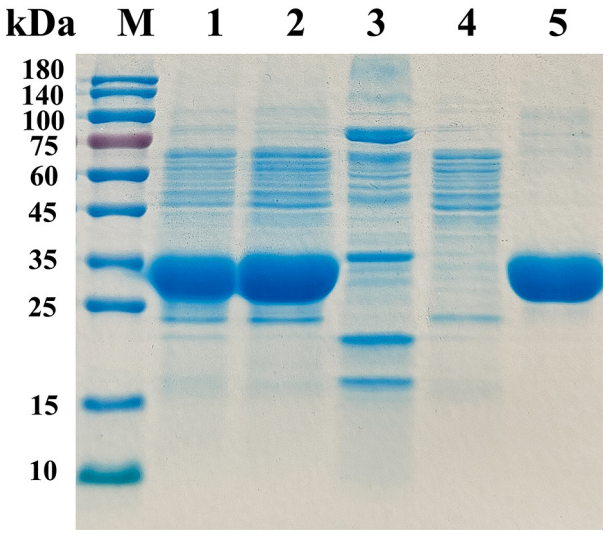

Fig. 5 Expression and purification analysis of Est1404 by SDS-PAGE. Lane M: protein molecular weight marker; lane 1: crude enzyme extract; lane 2: soluble fraction; lane 3: inclusion bodies; lane 4: flowthrough fraction; lane 5: purified protein elution.

Citation: *Polar Research* 2026, *45*, 10747, http://dx.doi.org/10.33265/polar.v45.10747

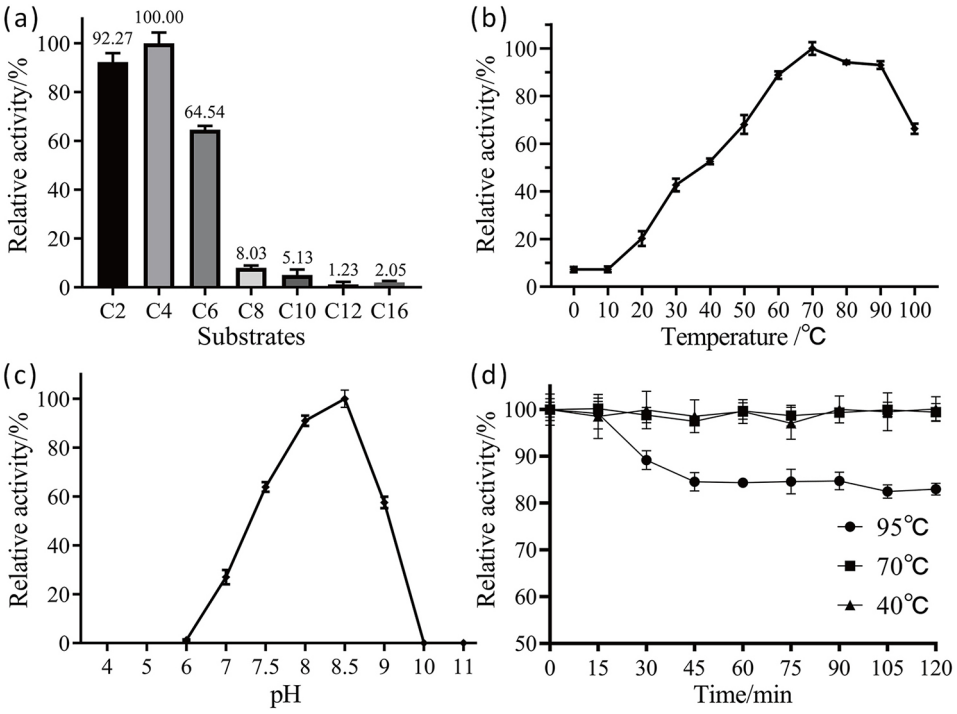

Fig. 6 Biochemical characterization of Est1404. (a) Substrate specificity. (b) Effect of temperature on the activity of Est1404. (c) Effect of pH on the activity of Est1404. (d) Thermostability assay. The enzyme was incubated at 40, 70 and 95 °C for different times and then residual activity was measured. The highest activity under optimal conditions was defined as 100%. Data represent mean values from three independent experiments. Data are presented as the mean ± SD of three independent biological replicates. Each biological replicate was measured in triplicate.

hydrolyse short-chain acyl compounds, showing the highest catalytic activity towards *p*NP-C4.

It is well known that Antarctic samples are suitable for isolating and discovering enzymes with cold adaptability. For example, esterase M-Est identified from the Antarctic bacterium *Marinomonas* sp. ef1. was highly thermolabile and active at low temperatures such as 5 °C (Marchetti et al. 2023). Furthermore, we previously identified an esterase, Est19, from *Pseudomonas* sp. E2–15 that belongs to a subfamily of the HSL. Est19 proved to be a cold-adaptive enzyme. It maintained almost full activity within a temperature range of 10–60 °C and retained approximately 50% of its activity at 0 °C (Liu, Zhou et al. 2021). In this study, however, Est1404 behaved like a thermophilic alkaline esterase, which exhibited its highest activity at a temperature of 70 °C and a pH of 8.5. This high optimal temperature is an unusual feature for an enzyme derived from a psychrophilic organism, yet such a phenomenon is not without precedent. For instance, a thermostable aldehyde dehydrogenase with a high temperature optimum (55–60 °C) has been identified in the Antarctic psychrophile *Cytophaga* sp. KUC-1 (Yamanaka et al. 2002), which grows optimally at 15 °C, demonstrating that the occurrence of thermophilic enzymes in cold-adapted hosts, though rare, is possible.

Furthermore, it demonstrated notable thermal resilience when exposed to high temperatures. Structural comparisons with Est19 revealed that Est1404 exhibits a more compact active site architecture and enhanced hydrogen bond networks, features that likely contribute to its thermostability. The reduced active site volume (370 Å³ in Est1404 vs. 600 Å³ in Est19) may enhance structural rigidity by limiting conformational flexibility and reducing the entropy of the unfolded state, thereby increasing the energy barrier for denaturation. This phenomenon is consistent with previous studies indicating that smaller and more compact active sites can improve thermostability through improved packing and reduced solvent accessibility, which minimizes destabilizing fluctuations at elevated temperatures (Feller & Gerday 2003; Unsworth et al. 2007). Additionally, the extended hydrogen bond network (20 interactions in Est1404 versus 18 in Est19) further stabilizes the tertiary structure around the catalytic residues (Li et al. 2005).

However, this increased rigidity comes at the cost of catalytic efficiency at lower temperatures, as reflected in Est1404's significantly lower k_{cat} (1.47 s^{-1}) and catalytic efficiency k_{cat}/K_m (7.9 $s^{-1}mM^{-1}$) compared to Est19 (21.86 s^{-1} and 148.68 $s^{-1}mM^{-1}$). This trade-off between stability and activity is a hallmark of thermal adaptation

Table 2 Relative activity percentage of Est1404 in the presence of additives. Data are presented as the mean ± SD of three independent biological replicates. Each biological replicate was measured in triplicate.

Additive	Residual activity (%)	
Inhibitors		
	1 mM	10 mM
EDTA	93.9 ± 12.8	102.1 ± 5.44
PMSF	97.97 ± 3.77	6.367 ± 3.03
DTT	299.2 ± 16.62	392.9 ± 18.5
	1% (w/v)	5% (w/v)
SDS	30.87 ± 9.72	0.9688 ± 0.80
Tween-80	49.17 ± 12.47	18.98 ± 1.52
CTAB	173.7 ± 45.08	149.2 ± 17.05
Organic reagents		
	20% (v/v)	40% (v/v)
Methanol	107.1 ± 7.17	56.71 ± 12.81
Formaldehyde	0	0
Ethanol	99.65 ± 14.17	42.12 ± 16.44
Acetonitrile	45.82 ± 4.65	0
Acetone	60.14 ± 8.16	22.24 ± 5.66
Isopropanol	78.95 ± 3.63	20.88 ± 7.72
DMSO	40.72 ± 6.59	9.534 ± 17.64
DMF	68.8 ± 2.09	29.53 ± 1.56

in enzymes (Johns & Somero 2004; Somero 2004). Despite its lower turnover, Est1404 maintains functional advantage at high temperatures (70 °C), where its rigid structure preserves active site integrity and substrate binding capability, whereas the more flexible Est19 would be prone to denaturation and loss of function. This adaptive strategy aligns with the mechanisms observed in other thermophilic enzymes, such as lactate dehydrogenases adapted to extreme thermal environments, which also exhibit reduced conformational flexibility to maintain catalytic function under thermal stress (Coquelle et al. 2007). Taken together, the structural basis for Est1404's thermostability, including its compact active site and enhanced hydrogen bond network, appears to be an intrinsic property of the enzyme. This marked discrepancy between the psychrophilic nature of the host organism and the thermophilic character of its encoded enzyme highlights the complex relationship between genomic content and phenotypic traits in environmental microorganisms.

Many thermophilic enzymes within the HSL family have been described in the literature. These include the following: E69 (optimal temperature 60 °C, ideal pH 10.5; Huo et al. 2017), EstD11 (optimal temperature 60 °C, optimal pH 8.0; Miguel-Ruano et al. 2021) and E25 (optimal temperature 45 °C, optimal pH 9.5; Rong et al. 2018). In addition, there are several HSL family esterases, such as Est1 (Tirawongsaroj et al. 2008) and EST2 (Manco et al. 1998), that display optimal activity and resilience at temperatures approaching 70 °C. However, the temperature profile and thermal stability of Est1404 proved to be much higher compared to those other thermophilic esterases. This suggests that Est1404 exhibited beneficial properties that might make it useful for industrial reactions that necessitate hydrolytic activity at temperatures over 50 °C or more (Munoz et al. 2015) for prolonged times. These thermostable properties enable potential applications in biodiesel production through transesterification, and in food processing for lipid modification under thermal treatment. The thermal stability improves efficiency in high-temperature organic synthesis, offering better reaction kinetics and product yields compared to typical esterases (Jin et al. 2019).

The enzyme activity of Est1404 was affected by the presence of specific chemical inhibitors and organic solvents. For example, PMSF is known to chemically modify active site serine residues (Gupta et al. 2004), resulting in the inhibition of esterase activity. In the present study, the addition of 10 mM PMSF resulted in near-total inhibition of Est1404 activity. These results suggest that Est1404 can be classified as a serine hydrolase. This is consistent with the results of sequence analysis and phylogenetic tree, indicating that Est1404 was a member of the GDSAG subfamily within the HSL family. The addition of DTT did not inhibit the activity of Est1404, suggesting the catalytic activity did not require disulfide bonds. These observations are consistent with previous reports that ester hydrolases are not affected by DTT, such as esterase LipA and thermophilic lipase from *Geobacillus* sp. TW1 (Snellman et al. 2002; Li & Zhang 2005). However, unlike these enzymes, the activity of Est1404 was enhanced about threefold by DTT. The significant activation suggests a distinct redox-sensitive regulatory mechanism. Based on our structural analysis, we speculate that oxidation of non-catalytic cysteines such as Cys^{38} and Cys^{282} near the substrate-binding pocket could induce conformational constraints that impair substrate access, while DTT-mediated reduction restores optimal binding geometry (Yao et al. 2012).

Furthermore, the significant enhancement of Est1404 activity by CTAB (50–70%) is likely due to a combination of structural and interfacial effects. The cationic head group of CTAB may interact with negatively charged residues on the enzyme surface, stabilizing its active conformation, while its hydrophobic tail could promote lid-opening, thereby exposing the catalytic site. Additionally, CTAB micelles may improve substrate accessibility by solubilizing hydrophobic substrates (Holmberg 2018). Similar activation has been reported for other lipases such as *Pachira aquatica* lipase (Polizelli et al. 2008).

The observed variations in residual enzyme activity across different organic reagents and concentrations can

Citation: *Polar Research* 2026, *45*, 10747, http://dx.doi.org/10.33265/polar.v45.10747

be attributed to their distinct interactions with the enzyme's structure. Formaldehyde completely inactivates the enzyme because its strong cross-linking ability leads to irreversible denaturation. Acetonitrile and DMSO cause significant activity loss at higher concentrations due to their high polarity disrupting essential hydrogen bonds and hydrophobic interactions. Methanol and ethanol show mild activation at low concentrations but destabilize the enzyme at higher levels, likely by perturbing hydration shells. Acetone, isopropanol and DMF partially inhibit activity, suggesting competitive binding or non-specific structural interference (Mohtashami et al. 2019; Dudkaitė et al. 2023).

Est1404, along with our previously characterized esterases Est19 and Est33 (Liu et al. 2022), were derived from *Pseudomonas* sp. E2–15 and *Pseudomonas* sp. E5–12 strains isolated from King George Island. These enzymes exhibit distinct temperature characteristics: Est1404 maintains over 90% activity between 60 and 90 °C, Est19 retains approximately 50% activity at 0 °C and Est33 demonstrates optimal activity at 30 °C with more than 50% activity preserved between 30 and 50 °C. This functional divergence likely stems from adaptations to permafrost environments, which exhibits high variability in temperature and water content in the summer, resulting in frequent freeze–thaw cycles (Schaefer et al. 2023). The presence of multiple enzyme variants with different thermal characteristics may enable microbial growth across wider temperature ranges. In *Pseudomonas* sp. E2–15, Est19 likely supports basal metabolism under cold conditions, whereas Est1404 may function during localized warming events caused by solar heating of dark soils, thereby enhancing metabolic flexibility. Alternatively, the *est1404* gene could represent a functional relic from an ancestor that inhabited a warmer environment. The precise ecological roles and adaptive advantages of maintaining such a diverse suite of esterases within a single habitat remain speculative and warrant further investigation.

Conclusion

Overall, both Est1404 and several previously identified thermophilic esterases belonging to the HSL family mostly exhibit characteristics of alkaline esterases. They demonstrate significant activity and durability at higher temperatures. This study provides a foundation for exploring the application of Est1404 in industrial processes and biotechnology.

Disclosure statement

The authors declare no conflict of interest.

Funding

The authors would like to acknowledge the funding from the Natural Science Foundation of Shandong Province, China (grant no. ZR2022MC153); the Science, Education and Industry Integration Innovation Pilot Project from Qilu University of Technology (Shandong Academy of Sciences; grant no. 2022PY061); and State Key Laboratory of Microbial Technology Open Projects Fund China (grant no. M2023-18).

Data availability

The *est1404* gene sequence that supports the findings of this study has been deposited in GenBank with the accession number OR876274. The whole genome shotgun sequencing project of the source strain, *Pseudomonas* sp. E2–15, has been deposited in GenBank (accession no. JBSKFM000000000, locus JBSKFM010000000). It has also been deposited in the Genome Warehouse of the National Genomics Data Center, Beijing Institute of Genomics, Chinese Academy of Sciences and China National Center for Bioinformation (accession no. GWHHCKT00000000.1), where it is publicly accessible (https://ngdc.cncb.ac.cn/gwh).

References

Almagro Armenteros J.J., Tsirigos K.D., Sønderby C.K., Petersen T.N., Winther O., Brunak S., von Heijne G. & Nielsen H. 2019. SignalP 5.0 improves signal peptide predictions using deep neural networks. *Nature Biotechnology 374*, 420–423, doi: 10.1038/s41587-019-0036-z.

Arnling Bååth J., Mazurkewich S., Poulsen J.N., Olsson L., Lo Leggio L. & Larsbrink J. 2019. Structure-function analyses reveal that a glucuronoyl esterase from *Teredinibacter turnerae* interacts with carbohydrates and aromatic compounds. *Journal of Biological Chemistry 294*, 6635–6644, doi: 10.1074/jbc.RA119.007831.

Arpigny J.L. & Jaeger K.E. 1999. Bacterial lipolytic enzymes: classification and properties. *Biochemical Journal 343*, 177–183, doi: 10.1042/bj3430177.

Ashaolu T.J., Malik T., Soni R., Prieto M.A. & Jafari S.M. 2025. Extremophilic microorganisms as a source of emerging enzymes for the food industry: a review. *Food Science & Nutrition 13*, e4540, doi: 10.1002/fsn3.4540.

Bornscheuer U.T. 2002. Microbial carboxyl esterases: classification, properties and application in biocatalysis. *FEMS Microbiology Reviews 26*, 73–81, doi: 10.1111/j.1574-6976.2002.tb00599.x.

Bredai R., Belhaj Ben Romdhane I., Bouchaala I., Srih Belghith K. & Belghith H. 2021. Purification of *Bacillus licheniformis* lipase and its application as an additive in detergent for destaining. *Journal of Surfactants and Detergents 24*, 835–853, doi: 10.1002/jsde.12514.

Bruins M.E., Janssen A.E.M. & Boom R.M. 2001. Thermozymes and their applications. *Applied Biochemistry and Biotechnology 90*, 155–186, doi: 10.1385/ABAB:90:2:155.

Coquelle N., Fioravanti E., Weik M., Vellieux F. & Madern D. 2007. Activity, stability and structural studies of lactate dehydrogenases adapted to extreme thermal environments. *Journal of Molecular Biology 374*, 547–562, doi: 10.1016/j.jmb.2007.09.049.

Corazza A., Rosano C., Pagano K., Alverdi V., Esposito G., Capanni C., Bemporad F., Plakoutsi G., Stefani M., Chiti F., Zuccotti S., Bolognesi M. & Viglino P. 2006. Structure, conformational stability, and enzymatic properties of acylphosphatase from the hyperthermophile *Sulfolobus solfataricus*. *Proteins 62*, 64–79, doi: 10.1002/prot.20703.

Curci N., Strazzulli A., De Lise F., Iacono R., Maurelli L., Dal Piaz F., Cobucci-Ponzano B. & Moracci M. 2019. Identification of a novel esterase from the thermophilic bacterium *Geobacillus thermodenitrificans* NG80-2. *Extremophiles 23*, 407–419, doi: 10.1007/s00792-019-01093-9.

D'Amico S., Sohier J.S. & Feller G. 2006. Kinetics and energetics of ligand binding determined by microcalorimetry: insights into active site mobility in a psychrophilic alpha-amylase. *Journal of Molecular Biology 358*, 1296–1304, doi: 10.1016/j.jmb.2006.03.004.

De Santi C., Ambrosino L., Tedesco P., de Pascale D., Zhai L., Zhou C., Xue Y. & Ma Y. 2015. Identification and characterization of a novel salt-tolerant esterase from a Tibetan glacier metagenomic library. *Biotechnology Progress 31*, 890–899, doi: 10.1002/btpr.2096.

Dudkaitė V., Kairys V. & Bagdžiūnas G. 2023. Understanding the activity of glucose oxidase after exposure to organic solvents. *Journal of Materials Chemistry B 11*, 2409–2416, doi: 10.1039/D2TB02605H.

Feller G. 2013. Psychrophilic enzymes: from folding to function and biotechnology. *Scientifica (Cairo) 2013*, article no. 512840, doi: 10.1155/2013/512840.

Feller G. & Gerday C. 2003. Psychrophilic enzymes: hot topics in cold adaptation. *Nature Reviews Microbiology 1*, 200–208, doi: 10.1038/nrmicro773.

Feller G., Lonhienne T., Deroanne C., Libioulle C., Van Beeumen J. & Gerday C. 1992. Purification, characterization, and nucleotide sequence of the thermolabile alpha-amylase from the antarctic psychrotroph *Alteromonas haloplanctis* A23. *Journal of Biological Chemistry 267*, 5217–5221, doi: 10.1016/S0021-9258(18)42754-8.

Ferruz N., Schmidt S. & Höcker B. 2021. ProteinTools: a toolkit to analyze protein structures. *Nucleic Acids Research 49*, W559–W566, doi: 10.1093/nar/gkab375.

Gasteiger E., Hoogland C., Gattiker A., Duvaud S., Wilkins M.R., Appel R.D. & Bairoch A. 2005. Protein identification and analysis tools on the ExPASy server. In J.M. Walker (ed.): *The proteomics protocols handbook*. Pp. 571–607. Totowa, NJ: Humana Press.

Gupta R., Gupta N. & Rathi P. 2004. Bacterial lipases: an overview of production, purification and biochemical properties. *Applied Microbiology and Biotechnology, 64*, 763–781, doi: 10.1007/s00253-004-1568-8.

Holmberg K. 2018. Interactions between surfactants and hydrolytic enzymes. *Colloids and Surfaces B: Biointerfaces 168*, 169–177, doi: 10.1016/j.colsurfb.2017.12.002.

Huo Y.Y., Rong Z., Jian S.L., Xu C.D., Li J. & Xu X.W. 2017. A novel halotolerant thermoalkaliphilic esterase from marine bacterium *Erythrobacter seohaensis* SW-135. *Frontiers in Microbiology 8*, article no. 2315, doi: 10.3389/fmicb.2017.02315.

Jeanmougin F., Thompson J.D., Gouy M., Higgins D.G. & Gibson T.J. 1998. Multiple sequence alignment with Clustal X. *Trends in Biochemical Sciences 23*, 403–405, doi: 10.1016/S0968-0004(98)01285-7.

Jiang H., Zhang S., Gao H. & Hu N. 2016. Characterization of a cold-active esterase from *Serratia* sp. and improvement of thermostability by directed evolution. *BMC Biotechnology 16*, article no. 7, doi: 10.1186/s12896-016-0235-3.

Jin M., Gai Y., Guo X., Hou Y. & Zeng R. 2019. Properties and applications of extremozymes from deep-sea extremophilic microorganisms: a mini review. *Marine Drugs 17*, article no. 656, doi: 10.3390/md17120656.

Jochens H., Hesseler M., Stiba K., Padhi S.K., Kazlauskas R.J. & Bornscheuer U.T. 2011. Protein engineering of *α/β* -hydrolase fold enzymes. *ChemBioChem 12*, 1508–1517, doi: 10.1002/cbic.201000771.

Johns G.C. & Somero G.N. 2004. Evolutionary convergence in adaptation of proteins to temperature: A4-lactate dehydrogenases of Pacific damselfishes (*Chromis* spp.). *Molecular Biology and Evolution 21*, 314–320, doi: 10.1093/molbev/msh021.

Kim B.Y., Yoo W., Le L.T.H.L., Kim K.K., Kim H.W., Lee J.H., Kim Y.O. & Kim T.D. 2019. Characterization and mutation analysis of a cold-active bacterial hormone-sensitive lipase from *Salinisphaera* sp. P7-4. *Archives of Biochemistry and Biophysics 663*, 132–142. doi: 10.1016/j.abb.2019.01.010.

Kim T.D. 2017. Bacterial hormone-sensitive lipases (bHSLs): emerging enzymes for biotechnological applications. *Journal of Microbiology and Biotechnology 27*, 1907–1915. doi: 10.4014/jmb.1708.08004.

Kovačić F., Babić N., Krauss U. & Jaeger K.-E. 2018. Classification of lipolytic enzymes from bacteria. In F. Rojo (ed.): *Aerobic utilization of hydrocarbons, oils and lipids*. Pp. 1–35. Cham: Springer.

Le L.T.H.L., Yoo W., Lee C., Wang Y., Jeon S., Kim K.K., Lee J.H. & Kim T.D. 2019. Molecular characterization of a novel cold-active hormone-sensitive lipase (HaHSL) from *Halocynthiibacter arcticus*. *Biomolecules 9*, article no. 704, doi: 10.3390/biom9110704.

Li H. & Zhang X. 2005. Characterization of thermostable lipase from thermophilic *Geobacillus* sp. TW1. *Protein Expression and Purification 42*, 153–159, doi: 10.1016/j.pep.2005.03.011.

Li P.Y., Ji P., Li C.Y., Zhang Y., Wang G.L., Zhang X.Y., Xie B.B., Qin Q.L., Chen X.L., Zhou B.C. & Zhang Y.Z. 2014. Structural basis for dimerization and catalysis of a novel esterase from the GTSAG motif subfamily of the bacterial hormone-sensitive lipase family. *Journal of Biological Chemistry 289*, 19031–19041, doi: 10.1074/jbc.M114.574913.

Li P.Y., Zhang Y.Q., Zhang Y., Jiang W.X., Wang Y.J., Zhang Y.S., Sun Z.Z., Li C.Y., Zhang Y.Z., Shi M., Song X.Y., Zhao L.S. & Chen X.L. 2020. Study on a novel cold-active and halotolerant monoacylglycerol lipase widespread in marine bacteria reveals a new group of bacterial monoacylglycerol lipases containing unusual C(A/S)HSMG catalytic motifs. *Frontiers in Microbiology 11*, article no. 9, doi: 10.3389/fmicb.2020.00009.

Li W.F., Zhou X.X. & Lu P. 2005. Structural features of thermozymes. *Biotechnology Advances 23*, 271–281, doi: 10.1016/j.biotechadv.2005.01.002.

Lima I.G.O., Bispo J.R.S., Agostinho A.Y.H., Queiroz A.C., Moreira M.S.A., Passarini M.R.Z., Oliveira V.M., Sette L.D., Rosa L.H. & Duarte A.W.F. 2022. Antarctic environments as a source of bacterial and fungal therapeutic enzymes. *Anais da Academia Brasileira de Ciências 94*, e20210452, doi: 10.1590/0001-3765202220210452.

Liu J., Liu W., Xing S., Zhang X., He H., Chen J., Bielicki J.K. & Zhou M. 2021. Diversity of protease-producing bacteria in the soils of the South Shetland Islands, Antarctica. *Antonie van Leeuwenhoek 114*, 457–464, doi: 10.1007/s10482-021-01533-7.

Liu X., Zhou M., Sun R., Xing S., Wu T., He H., Chen J. & Bielicki J.K. 2022. Characterization of a novel esterase Est33 from an Antarctic bacterium: a representative of a mew esterase family. *Frontiers in Microbiology 13*, article no. 855658, doi: 10.3389/fmicb.2022.855658.

Liu X., Zhou M., Xing S., Wu T., He H., Bielicki J.K. & Chen J. 2021. Identification and biochemical characterization of a novel hormone-sensitive lipase family esterase Est19 from the Antarctic bacterium *Pseudomonas* sp. E2-15. *Biomolecules 11*, article no. 1552, doi: 10.3390/biom11111552.

Liu Y., Liu R., Mou Y. & Zhou G. 2011. Spectroscopic identification of interactions of formaldehyde with bovine serum albumin. *Journal of Biochemical and Molecular Toxicology 25*, 95–100, doi: 10.1002/jbt.20364.

Manco G., Adinolfi E., Pisani F.M., Ottolina G., Carrea G. & Rossi M. 1998. Overexpression and properties of a new thermophilic and thermostable esterase from *Bacillus acidocaldarius* with sequence similarity to hormone-sensitive lipase subfamily. *Biochemical Journal 332*, 203–212, doi: 10.1042/bj3320203.

Marchetti A., Orlando M., Mangiagalli M. & Lotti M. 2023. A cold-active esterase enhances mesophilic properties through Mn^{2+} binding. *FEBS Journal 290*, 2394–2411, doi: 10.1111/febs.16661.

Miguel-Ruano V., Rivera I., Rajkovic J., Knapik K., Torrado A., Otero J.M., Beneventi E., Becerra M., Sánchez-Costa M., Hidalgo A., Berenguer J., González-Siso M.I., Cruces J., Rúa M.L. & Hermoso J.A. 2021. Biochemical and structural characterization of a novel thermophilic esterase EstD11 provide catalytic insights for the HSL family. *Computational and Structural Biotechnology Journal 19*, 1214–1232, doi: 10.1016/j.csbj.2021.01.047.

Mogodiniyai Kasmaei K. & Sundh J. 2019. Identification of novel putative bacterial feruloyl esterases from anaerobic ecosystems by use of whole-genome shotgun metagenomics and genome binning. *Frontiers in Microbiology 10*, article no. 2673, doi: 10.3389/fmicb.2019.02673.

Mohtashami M., Fooladi J., Haddad-Mashadrizeh A., Housaindokht M.R. & Monhemi H. 2019. Molecular mechanism of enzyme tolerance against organic solvents: insights from molecular dynamics simulation. *International Journal of Biological Macromolecules 122*, 914–923, doi: 10.1016/j.ijbiomac.2018.10.172.

Munoz P.A., Correa-Llanten D.N. & Blamey J.M. 2015. Ionic liquids increase the catalytic efficiency of a lipase (Lip1) from an antarctic thermophilic bacterium. *Lipids 50*, 49–55, doi: 10.1007/s11745-014-3973-9.

Petrovskaya L.E., Novototskaya-Vlasova K.A., Spirina E.V., Durdenko E.V., Lomakina G.Y., Zavialova M.G., Nikolaev E.N. & Rivkina E.M. 2016. Expression and characterization of a new esterase with GCSAG motif from a permafrost metagenomic library. *FEMS Microbiology Ecology 92*, fiw046, doi: 10.1093/femsec/fiw046.

Piroozmand F., Ghadam P., Zarrabi M. & Abdi-Ali A. 2020. Biochemical and computational study of an alginate lyase produced by *Pseudomonas aeruginosa* strain S21. *Iranian Journal of Basic Medical Sciences 23*, 454–460, doi: 10.22038/ijbms.2020.37277.8874.

Polizelli P.P., Tiera M.J. & Bonilla-Rodriguez G.O. 2008. Effect of surfactants and polyethylene glycol on the activity and stability of a lipase from oilseeds of *Pachira aquatica*. *Journal of the American Oil Chemists' Society 8*5, 749–753, doi: 10.1007/s11746-008-1259-1.

Reyes-Reyes A.L., Valero Barranco F. & Sandoval G. 2022. Recent advances in lipases and their applications in the food and nutraceutical industry. *Catalysts 12*, article no. 960, doi: 10.3390/catal12090960.

Robert X. & Gouet P. 2014. Deciphering key features in protein structures with the new ENDscript server. *Nucleic Acids Research 42*, W320–W324, doi: 10.1093/nar/gku316.

Rong Z., Huo Y.Y., Jian S.L., Wu Y.H. & Xu X.W. 2018. Characterization of a novel alkaline esterase from *Altererythrobacter epoxidivorans* CGMCC 1.7731^T. *Preparative Biochemistry and Biotechnology 48*, 113–120, doi: 10.1080/10826068.2017.1387559.

Schaefer C.E.G.R., Francelino M.R., Pereira A.B., Michel R.F.M., Schmitz D., Sacramento I.F., Rodrigues W.F. & Miranda C.O. 2023. Thermal monitoring of a Cryosol in a high marine terrace (Half Moon Island, Maritime Antarctica). *Anais da Academia Brasileira de Ciências 95(Suppl. 3)*, e20210692, doi: 10.1590/0001-3765202320210692.

Sharma N., Ahlawat Y.K., Stalin N., Mehmood S., Morya S., Malik A., Malathi H., Nellore J. & Bhanot D. 2024. Microbial enzymes in industrial biotechnology: sources, production, and significant applications of lipases. *Journal of Industrial Microbiology and Biotechnology 52*, kuaf010, doi: 10.1093/jimb/kuaf010.

Snellman E.A., Sullivan E.R. & Colwell R.R. 2002. Purification and properties of the extracellular lipase, LipA, of *Acinetobacter* sp. RAG-1. *European Journal of Biochemistry 269*, 5771–5779, doi: 10.1046/j.1432-1033.2002.03235.x.

Somero G.N. 2004. Adaptation of enzymes to temperature: searching for basic "strategies". *Comparative Biochemistry*

and Physiology Part B 139, 321–333, doi: 10.1016/j.cbpc.2004.05.003.

Soumya P. & Kochupurackal J. 2022. An esterase with increased acetone tolerance from *Bacillus subtilis* E9 over expressed in *E. coli* BL21 using pTac Bs-est vector. *Molecular Biotechnology 64*, 814–824, doi: 10.1007/s12033-022-00458-4.

Stivala A., Wybrow M., Wirth A., Whisstock J.C. & Stuckey P.J. 2011. Automatic generation of protein structure cartoons with Pro-origami. *Bioinformatics 27*, 3315–3316, doi: 10.1093/bioinformatics/btr575.

Tamura K., Stecher G. & Kumar S. 2021. MEGA11: molecular evolutionary genetics analysis version 11. *Molecular Biology and Evolution 38*, 3022–3027, doi: 10.1093/molbev/msab120.

Tirawongsaroj P., Sriprang R., Harnpicharnchai P., Thongaram T., Champreda V., Tanapongpipat S., Pootanakit K. & Eurwilaichitr L. 2008. Novel thermophilic and thermostable lipolytic enzymes from a Thailand hot spring metagenomic library. *Journal of Biotechnology 133*, 42–49, doi: 10.1016/j.jbiotec.2007.08.046.

Tutuncu H.E., Balci N., Tuter M. & Karaguler N.G. 2019. Recombinant production and characterization of a novel esterase from a hypersaline lake, Acigol, by metagenomic approach. *Extremophiles 23*, 507–520, doi: 10.1007/s00792-019-01103-w.

Unsworth L.D., van der Oost J. & Koutsopoulos S. 2007. Hyperthermophilic enzymes—stability, activity and implementation strategies for high temperature applications. *FEBS Journal 274*, 4044–4056, doi: 10.1111/j.1742-4658.2007.05954.x.

Vieille C. & Zeikus G.J. 2001. Hyperthermophilic enzymes: sources, uses, and molecular mechanisms for thermostability. *Microbiology and Molecular Biology Reviews 65*, 1–43, doi: 10.1128/mmbr.65.1.1-43.2001.

Wang Y., Xu Y., Zhang Y., Sun A. & Hu Y. 2018. Functional characterization of salt-tolerant microbial esterase WDEst17 and its use in the generation of optically pure ethyl (*R*)-3-hydroxybutyrate. *Chirality 30*, 769–776, doi: 10.1002/chir.22847.

Wu G., Zhang X., Wei L., Wu G., Kumar A., Mao T. & Liu Z. 2015. A cold-adapted, solvent and salt tolerant esterase from marine bacterium *Psychrobacter pacificensis*. *International Journal of Biological Macromolecules 81*, 180–187, doi: 10.1016/j.ijbiomac.2015.07.045.

Yamanaka Y., Kazuoka T., Yoshida M., Yamanaka K., Oikawa T. & Soda K. 2002. Thermostable aldehyde dehydrogenase from psychrophile, *Cytophaga* sp. KUC-1: enzymological characteristics and functional properties. *Biochemical and Biophysical Research Communications 298*, 632–637, doi: 10.1016/S0006-291X(02)02523-8.

Yang W., He Y., Xu L., Zhang H. & Yan Y. 2016. A new extracellular thermo-solvent-stable lipase from *Burkholderia ubonensis* SL-4: identification, characterization and application for biodiesel production. *Journal of Molecular Catalysis B: Enzymatic 126*, 76–89, doi: 10.1016/j.molcatb.2016.02.005.

Yao Z., Zhang C., Lu F., Bie X. & Lu Z. 2012. Gene cloning, expression, and characterization of a novel acetaldehyde dehydrogenase from *Issatchenkia terricola* strain XJ-2. *Applied Microbiology and Biotechnology 93*, 1999–2009, doi: 10.1007/s00253-011-3541-7.

Ye B., Tian W., Wang B. & Liang J. 2024. CASTpFold: computed atlas of surface topography of the universe of protein folds. *Nucleic Acids Research 52*, W194–W199, doi: 10.1093/nar/gkae415.

Yu N., Yang J.C., Yin G.T., Li R.S., Zou W.T. & He C. 2018. Identification and characterization of a novel esterase from *Thauera* sp. *Biotechnology and Applied Biochemistry 65*, 748–755, doi: 10.1002/bab.1659.

Zhang H., Li M., Li J., Wang G. & Liu Y. 2017. Purification and properties of a novel quizalofop-*p*-ethyl-hydrolyzing esterase involved in quizalofop-*p*-ethyl degradation by *Pseudomonas* sp. J-2. *Microbial Cell Factories 16*, article no. 80, doi: 10.1186/s12934-017-0695-8.

Zhang Y., Ji F., Wang J., Pu Z., Jiang B. & Bao Y. 2018. Purification and characterization of a novel organic solvent-tolerant and cold-adapted lipase from *Psychrobacter* sp. ZY124. *Extremophiles 22*, 287–300, doi: 10.1007/s00792-018-0997-8.

Zhao J., Ma M., Zeng Z., Yu P., Gong D. & Deng S. 2021. Production, purification and biochemical characterisation of a novel lipase from a newly identified lipolytic bacterium *Staphylococcus caprae* NCU S6. *Journal of Enzyme Inhibition and Medicinal Chemistry 36*, 248–256, doi: 10.1080/14756366.2020.1861607.